4E2-3

Impact of Frequency-Selective High-Impedance Surface Reflectors on Directivity of Ultra-wideband Monopole Antennas

#Koji Inafune, Hiroshi Osabe, and Eiichi Sano
Research Center for Integrated Quantum Electronics, Hokkaido University
North 13 West 8, Sapporo 060-8628, Japan, e-mail: inafune@rciqe.hokudai.ac.jp

1. Introduction

Ultra-wideband (UWB) systems with a band of 3.1-10.6 GHz are attractive for wireless personal area networks (PAN). The need for smaller and low profile broadband antennas has become increasingly important as UWB equipment is miniaturized. Maltiple types of wideband antennas have been proposed for UWB systems [1, 2]. Most of them are measured in free space. However, when an antenna is mounted in wireless equipment, the other equipment, such as the printed circuit boards, affects the antenna's performance.

Metamaterials, such as left-handed (negative refractive index) materials [3], have unique electromagnetic properties that are very useful in producing new functional devices. Frequency-selective high-impedance surfaces (FSHIS), one type of metamaterial, have frequency-dependent reflection phase characteristics and act as a magnetic wall at a specified frequency. This property makes it possible to use FSHIS as antenna reflectors. Two major structures have been proposed to fabricate FSHIS. One has a two-dimensional microstrip patch array with a conducting via that connects the center of each patch to the backside metal plane [4]. The other structure eliminates the vias from the array [5]. Reports on the effects of FSHISs on wire and patch antennas reveal that FSHISs enhance antenna efficiency, making it possible to reduce the size of the antennas [4-7]. The antennas used so far have had relatively narrow bandwidths.

This paper reports on the impact of FSHIS reflectors on UWB antenna performance. Section 2 describes the structures of UWB antennas and FSHISs. Section 3 discusses the reflection phase and dispersion characteristics of the two kinds of FSHIS (with and without vias) simulated using the finite-difference time-domain (FDTD) method. It also discusses the frequency dependence of antenna gains on FSHIS reflectors. Section 4 presents measurements of antenna and FSHIS characteristics that confirm the simulated results.

2. Configuration of antenna and FSHIS reflector

The compact microstrip-fed monopole antenna shown on the left side of Fig. 1(a) was chosen for use as a wide band antenna because its structure is typical of such antennas. It is identical with the antenna proposed in [2], except that it has no quarter wavelength U-shaped slot for a band-stop filter. The geometry is optimized to obtain low return loss from 3.1 to 11.24 GHz [2].

The monopole antenna should be incorporated with the FSHIS reflector to transmit unilateral hemisphere radiation. Both kinds of FSHIS reflector described in Section 1 are investigated in this study. The space period and gap are 2.4 and 0.15 mm, respectively. One has 0.36-mm wide vias, as shown on the right side of Fig. 1(b), and the other has no vias.

The antenna and the FSHISs were fabricated on 1.6-mm thick FR4 substrate with a relative dielectric constant of 4.4. To fix the antenna height, FR4 substrate is inserted as spacer between the antenna ground plane and the FSHIS, as shown in Fig. 1(b). The height of the antenna in the patch arrays is 3.2 mm, which corresponds to 0.1λ at 5 GHz, where λ is the wavelength in the FR4 substrate.

3. Design of antenna placed over FSHIS reflector

ISBN: 978-4-88552-223-9 C3055©IEICE

3.1 Reflection phase and dispersion characteristics for the FSHIS reflector

The FSHIS covering the FR4 substrate was analyzed using the FDTD electromagnetic field simulator implementing the periodic boundary condition. The phase shifts between neighbouring unit cells $\exp(-jk_xL)$ and $\exp(-jk_yL)$ were translated from the frequency to the time domain using the sine-cosine method [8].

Figure 2 shows the reflection phase characteristics for both FSHISs with the normally incident plane wave, which means $k_x=k_y=0$. The resonance frequency is located in the center of EBG [4]. The in-phase range also corresponds to EBG [4]. It was expected that the resonance frequency of the FSHISs with and without vias would be 6.96 and 6.78 GHz, respectively. Both FSHIS structures and their geometries, shown in Fig. 1(a), have similar phase characteristics.

Figure 3 shows the dispersion characteristics for both FSHISs. The fundamental and next higher modes are TM and TE surface wave modes, respectively. Both FSHIS structures exhibit similar characteristics for the TE mode, which monotonically increases as wavenumber increases. In contrast, dispersion curves for TM mode differ greatly from each other. The dispersion curve of the FSHIS without vias increases monotonically, just as the curve for the TE mode does. Therefore, the FSHIS without vias has no EBG, at least in the frequency range shown in Fig. 3. The FSHIS with vias has a maximum frequency at a certain wavenumber, and an extremely slow negative group velocity is indicated in almost the entire wave vector range. The maximum frequency is lower than the TE mode cut off frequency. Therefore FSHIS with vias has an EBG between 6.44 and 7.70 GHz.

3.2 Antenna gain

The antenna incorporated with the FSHIS reflector shown in Fig. 1 was analyzed using the FDTD method. The unit cells were assumed to be arranged in an 11 x 11 array due to the limited computational resources. The spacer, the substrate of the FSHIS, and the backside metal of the FSHIS were assumed to be spread infinitely. Figure 4 shows the actual gain versus frequency. The shaded frequency region is the EBG of the FSHIS with vias, which was analyzed using the FDTD method. The E_ϕ component in the θ=0 and ϕ=0 degrees is about 1 dBi between 4.2 and 9.0 GHz when the monopole antenna is not incorporated with the FSHIS reflector. The FSHIS without vias improves the E_ϕ component in the frequency range below 8 GHz, while the FSHIS with vias degrades it tremendously between 5.0 and 6.0 GHz. In addition, the FSHIS with vias causes the E_θ component in the θ=45 and ϕ=0 degrees to increase suddenly between 5.0 and 6.0 GHz. Figure 5 shows the directivity in the *zx* plane (ϕ=0 degree). The FSHIS with vias suppresses the undesired radiation along the patch plane at 7 GHz because of its EBG. Although the polarization of the monopole antenna is dominant in the E_ϕ component, the FSHIS with vias transforms it into the E_θ component at 5 GHz. The same tendency was expected from FDTD simulation when the broadband monopole antenna was replaced by a simple dipole antenna with a width and length of 1.18 mm and 21.6 mm, respectively (not shown here). Therefore, the frequency region with the degraded gain is mainly determined by FSHIS characteristics.

To investigate the reason for the extreme deterioration of the E_ϕ component, a current density distribution on the patch array, when the antenna is fed by a continuous wave source of 5 and 7 GHz, was calculated. Only the TM mode is excited because these frequencies are lower than the TE cut off frequency. At 7 GHz, FDTD simulations indicate that the current vector is directed parallel to the edge of the patch in both FSHISs, as shown in Fig. 6(a). At 5 GHz, it seems that the current density distribution is totally different between the two FSHISs, as shown in Fig. 6(b). The flat band of the TM mode may cause the difference because it enables the widely directional wave vector.

4. Measured results

An FSHIS with an 81 x 81 unit cell array was used in the measurements. Figure 7(a) shows the coupling degree between two antennas. Each antenna was connected to port 1 and port 2 of the vector network analyzer. It is similar to surface wave transmission characteristics [9], hence it is

possible to confirm the whether or not EBG occurs. The measurements indicate that the FSHIS with vias has an EBG between 7.6 and 9.0 GHz. It is speculated that the dispersion curve for the TM mode is flat at 7.6 GHz.

Figure 7(b) shows free space transmission in the θ=0 degree and ϕ=0 degree. The monopole antenna and the commercial horn antenna are connected with each port of the vector network analyzer. The distance from one to the other is about 27 cm. The FSHIS without vias enhances transmission between 5.0 and 9.1 GHz. The FSHIS with vias, in contrast, drastically degrades transmission at 7.6 GHz, which corresponds to the flat band frequency. These measurement results qualitatively agree with simulated results.

5. Conclusion

This paper reported on the impact of FSHIS reflectors on UWB monopole antenna performance. Both FDTD simulations and experiments exhibited a degraded gain in the direction of θ=0 and ϕ=0 when using an FSHIS with vias as a reflector. This is due to the fact that the fundamental TM mode becomes flat at a wide range of wavenumbers in the dispersion diagram for an FSHIS with vias. In contrast, an FSHIS without vias enhanced antenna gain. These results indicate that the FSHIS structure should be optimized for each individual antenna geometry.

Acknowledgments

The authors would like to thank Prof. Kasai for supporting our measurements. This work was partly supported by a Grant-in-Aid for Scientific Research from the Japanese Ministry of Education, Culture, Sports, Science and Technology.

References

[1] H. -D. Chen, "Broadband CPW-fed square slot antennas with a widened tuning stub," *IEEE Trans. Antennas Propagat.*, vol. 51, pp. 1982-1986, Aug. 2003.

[2] W. Choi, J. Jung, K. Chung, and J. Choi, "Compact mictsrip-fed antenna with band-stop characteristic for ultra-wideband applications," *Microwave Optical Technol. Lett.*, vol. 47, pp. 89-92, Oct. 2005.

[3] C. Caloz, A. Sanada, and T. Itoh, "A novel composite right-/left-handed coupled-line directional coupler with arbitrary coupling level and broad bandwidth," *IEEE Trans. Microwave Theory Tech*., vol. 52, pp. 980-992, Mar. 2004.

[4] D. Sievenpiper, L. Zhang, R. F. J. Broas, N. G. Alexopolous, and E. Yablonovicth, "High-impedance electromagnetic surfaces with a forbidden frequency band," *IEEE Trans. Microwave Theory Tech*., vol. 47, pp. 2059-2074, Nov. 1999.

[5] Y. Zhang, J. von Hagen, M. Younis, C. Fischer, and W. Wiesbeck, "Planar artificial magnetic conductors and patch antennas," *IEEE Trans. Antennas Propagat.*, vol. 51, pp. 2704-2712, Oct. 2003.

[6] R. C. Hansen, "Effect of a high-impedance screen on a dipole antenna," *IEEE Antennas Wireless Propagat. Lett*., vol. 1, pp. 46-49, 2002.

[7] M. F. Abedin and M. Ali, "Effects of EBG reflection phase profiles on the input impedance and bandwidth of ultrathin directional dipole," *IEEE Trans. Antennas Propagat.*, vol. 53, pp. 3664-3672, Nov. 2005.

[8] P. Harms, R. Mittra, and W. Ko,"Implementation of the periodic boundary condition in the finite-difference time-domain algolism for FSS structures," *IEEE Trans. Antennas Propagat*., vol. 42, pp. 1317-1324, Sep. 1994.

[9] C. Wang, D. –B. Yan, and N. –C. Yuan, "Application of high impedance electromagnetic surface to archimedean planner spiral antenna," *Microwave Optical Technol. Lett.*, vol. 49, pp. 129-131, Jan. 2007.

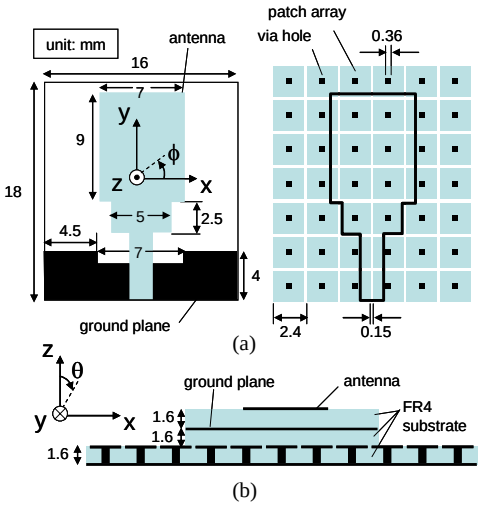

Fig. 1 Geometry of antenna and FSHIS. (a) top view

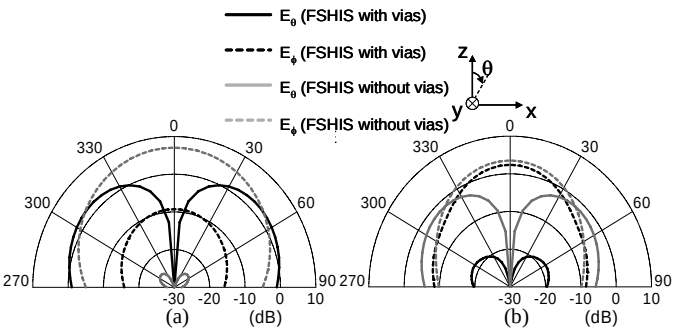

Fig. 5 Simulated directivity in *zx* plane at (a) 5 GHz and (b) 7 GHz.

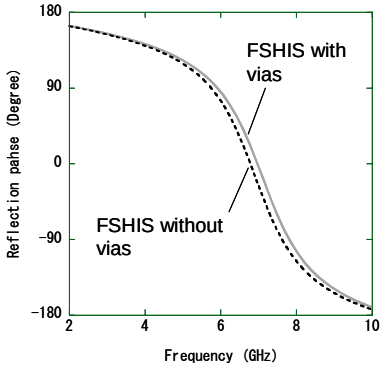

Fig. 2 Reflection phase characteristics.

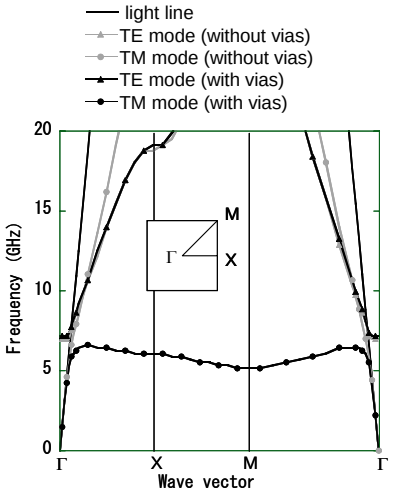

Fig. 3 Dispersion diagram.

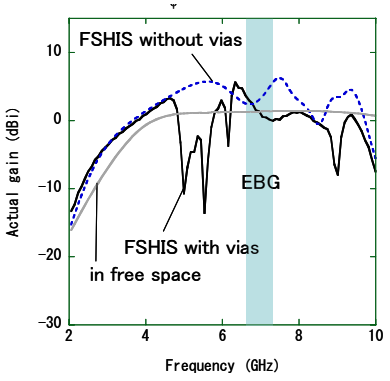

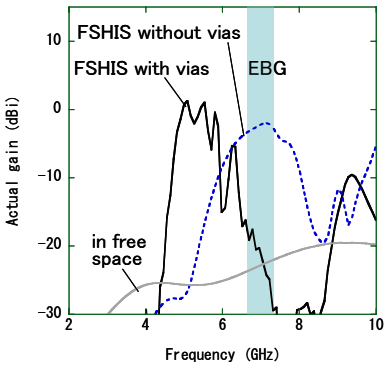

Fig. 4 Simulated actual gain. (a) E_ϕ component in θ=0 and ϕ=0 degrees. (b) E_θ component in θ=45 and ϕ=0 degrees.

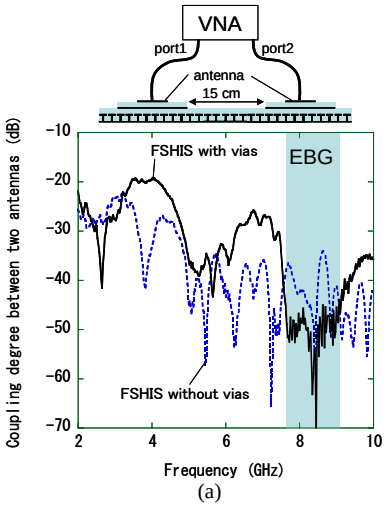

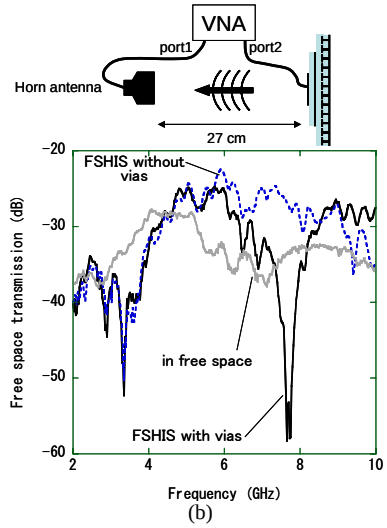

Fig. 7 Measured results. (a) coupling degree between two antennas. (b) free space transmission.

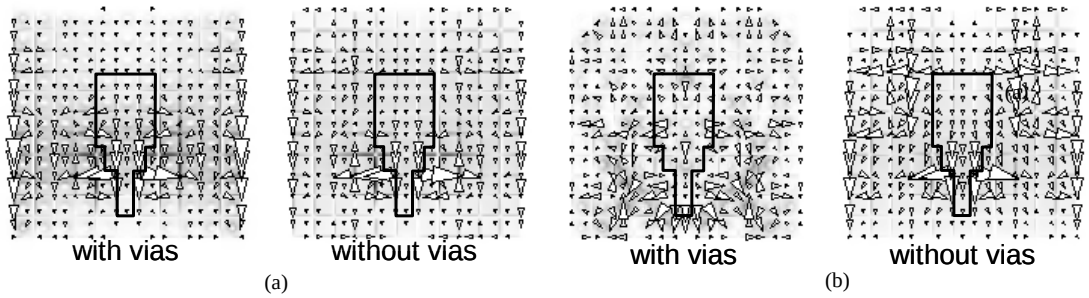

Fig. 6 Simulated current density distribution on patch array at (a) 7 GHz and (b) 5 GHz.